

# A novel combination of experimental design and artificial neural networks as an analytical tool for improving performance in thermospray flame furnace atomic absorption spectrometry

Ezequiel Morzan <sup>a</sup>, Jorge Stripeikis <sup>b</sup>, Hector Goicoechea <sup>c</sup>, Mabel Tudino <sup>a,\*</sup>

<sup>a</sup> Laboratorio de Análisis de Trazas. INQUIMAE, Departamento de Química Inorgánica, Analítica y Química Física, Universidad de Buenos Aires, Pabellón 2, Ciudad Universitaria, (1428) Buenos Aires, Argentina

<sup>b</sup> Departamento de Ingeniería Química, Instituto Tecnológico de Buenos Aires, Av Eduardo Madero 399 C1106, Buenos Aires, Argentina

<sup>c</sup> Laboratorio de Desarrollo Analítico y Quimiometría (LADAQ), Cátedra de Química Analítica I, Facultad de Bioquímica y Ciencias Biológicas, Universidad Nacional del Litoral-CONICET, C.C. 242, S3000ZAA Santa Fe, Argentina

## A B S T R A C T

In this work, we present the combined effect of artificial neural networks (ANN) and experimental design as a suitable analytical tool for improving the performance of thermospray flame furnace atomic absorption spectrometry (TS-FFAAS) using Mg as leading case.

To this end, mixtures of different amounts of methanol, ethanol, and i-propanol in water were assayed as carriers at different flow rates and different flame stoichiometries (air/acetylene ratios). Different levels of these variables determined the experimental domain, consisting in a cube which was divided into eight identical cubical regions that allowed increase in the number of available experimental points. A Box–Behnken design (BBD) was employed in each one of the regions. The name Multiple Box–Behnken design (MBBD) was given to this new approach. Then, the features of ANN were exploited to find the optimum conditions for conducting Mg determination by TS-FFAAS.

The prediction capability of ANN was examined and compared to the least-squares (LS) fitting when applied to the response surface method (RSM).

The suitability of the new approach and the implications on TS-FFAAS analytical performance are discussed.

## Keywords:

ANN

Experimental design

Thermospray flame furnace atomic absorption spectrometry

## 1. Introduction

Thermospray flame furnace atomic absorption spectrometry (TS-FFAAS) was first reported by Berndt et al. [1]. This method allows the introduction of the whole sample into the flame furnace with no clogging, together with an increased time of residence of the analyte in the furnace which improve limits of detection and sensitivities up to the  $\mu\text{g L}^{-1}$  level [2–5].

In a previous paper [6], the authors reported a good analytical sensitivity for Mg determination by TS-FFAAS. In this work, further optimization studies were performed in order to get the best analytical conditions for the determination and thus, optimal response.

Considering that the traditional one variable at a time method is not the best mean for finding optimal conditions, more advanced optimization approaches such as the multivariable approach [7] were evaluated on the knowledge that it allows to enhance sensitivity and save time

and reagents with the consequent decrease of costs. The implementation of the multivariate approach is known as response surface methodology (RSM) [8].

Experimental design and RSM have been proven to be useful for developing, improving, and optimizing a wide range of processes [9–21].

When RSM is applied, the experimental responses are usually fitted to quadratic or higher order functions by least squares (LS). In most cases studied by this methodology, a second-degree polynomial relation can reasonably approximate the behavior of the systems under study.

Artificial neural networks (ANN) represent another smart tool for non-linear multivariate modeling. It is a parallel distributed processor that has the capability for storing experimental knowledge, hence making it available for use. Due to its superior classification and prediction capabilities, ANN has found its impact in empirical model building. Nowadays, the use of artificial neural network (ANN) in combination with experimental design is employed in different areas of science [22–26]. Among the main advantages of ANN compared to LS, the former does not require a prior specification of a suitable fitting function and has universal approximation capability, i.e. it can approximate almost all kinds of non-linear functions, including quadratic functions.

\* Corresponding author. Tel.: +54 1145763360; fax: +54 1145763341.  
E-mail address: tudino@qi.fcen.uba.ar (M. Tudino).

LS, on the other hand, is only useful for quadratic approximations. Nonetheless, it should be noticed that more complex functions require a larger number of experiments [27].

In the present work, we modified the Box–Behnken design (BBD) by dividing the cube that defines the experimental domain in eight identical cubical zones in order to increase the sampling density and to obtain a more efficient screening of the mentioned experimental domain. The name Multiple Box–Behnken design (MBBD) was given to this new method. Then, we exploited the features of the ANN to find the optimum conditions for conducting the magnesium analysis by TS-FFAAS.

The results obtained with the combined approach were compared to RSM with LS fitting, showing a remarkable improvement in terms of prediction capability.

The new approach was employed to optimize the analytical signal of Mg—taken as leading case—with the aim to broaden TS capabilities to the determination of other elements not assayed yet. Special attention was given to the physicochemical parameters that influence the generation of the analytical signal and thus, the performance of TS-FFAAS determinations.

## 2. Experimental

### 2.1. Reagents and materials

All solutions were prepared with analytical grade chemical reagents and double deionized water (DIW) obtained from a Milli-Q purification system (Millipore, Bedford, MA, USA). All glassware was washed with EXTRAN (Merck) 1% v/v and kept in 10% (v/v) HCl with further cleaning with DDW. Magnesium standard solutions were prepared daily by appropriate dilutions of 1000 mg L<sup>-1</sup> stock standard solution (Merck). Organic solvents methanol, ethanol, i-propanol, were Merck P.A.

### 2.2. Apparatus

A flame atomic absorption spectrometer Shimadzu AAS 6800 (Kyoto, Japan) equipped with a hollow cathode lamp of magnesium as radiation source and a deuterium lamp for background correction was used. Instrumental conditions were those provided by the manufacturer. Transient signals were recorded in the peak height mode.

The TS-FFAAS system was assembled with a peristaltic pump of eight channels and six rollers (IPC, Ismatec, Glattbrugg-Zürich, Switzerland), a six-ports rotatory valve VICI (Valco Instruments, Houston, TX, USA), 0.5 mm i.d. PTFE® tubings, a ceramic capillary (0.5 mm i.d., 6 cm length), and a perforated (six holes) nickel flame furnace atomizer placed on an air/acetylene flame with the assistance of a homemade steel holder.<sup>6</sup> The nickel tube (Inconel 600® alloy, Camacam, São Paulo, Brazil) composition was > 72% wt Ni, 14–17% wt Cr, and 6–10% wt

Fe as major constituents. The dimensions were 9.7 mm i.d. and 100 mm length.

### 2.3. Neural network and least-squares optimization procedure

In this study, we investigated different concentrations of three alcohols in water as carriers, different carrier flow rates, and different acetylene flow rates (at constant air flow rate) for the determination of magnesium by TS-FFAAS. The levels of three independent variables were selected based on the previous data and a preliminary work [6]. A strategy derived from the Box–Behnken design (BBD) was employed to increase the number of sampling points. If we consider the experimental domain as a cube, a BBD is built as displayed in Fig. 1 where the thirteen colored points represent thirteen experimental runs. In this new approach, the whole experimental domain was divided into eight identical cubes and a BBD was performed in each one of them (see Fig. 1). In this way, a total of 62 experimental points were defined using this strategy which we named Multiple Box–Behnken Design (MBBD). Note that the volumes occupied by the eight cubes on the right (MBBD) and the one on the left (BBD) are the same. Fig. 1 shows a difference for a better understanding.

For modeling and prediction of the analytical sensitivity of magnesium by TS-FFAAS, ANN and LS were used. LS was applied fitting polynomials of different degrees and evaluating the coefficient models through ANOVA [8].

Parallel systems of simple processing elements, neurons, are interconnected to produce artificial neural network. In the present study, feed forward, multilayer perceptions (MLP) type of ANN was used to predict the optimum conditions. Training of the ANN was accomplished through the back-propagation algorithm in MLP, which is the most commonly used in supervised MLP. Three ANN were trained to predict the response surface of each one of the alcohols. In doing that, different network architectures were tested and the best prediction was obtained for a network of one hidden layer with 50 neurons for methanol and 60 neurons for the other solvents. The transfer function was a sigmoid. In the training procedure, the information was processed in the forward direction from the hidden layer to the output layer obtained as the output of the network.

The data were processed using Matlab 8.0 for artificial neural network. Design Expert™ version 8.05.0 (Stat-Ease, Inc., Minneapolis, USA, 2010) was used to perform experimental design and LS.

## 3. Results and discussion

ANN and LS fitting in combination with experimental design were applied for the optimization of Mg determination by TS-FFAAS with three water/alcohol mixtures: methanol, ethanol, and i-propanol, being the key variables that control sensitivity, the alcohol/water

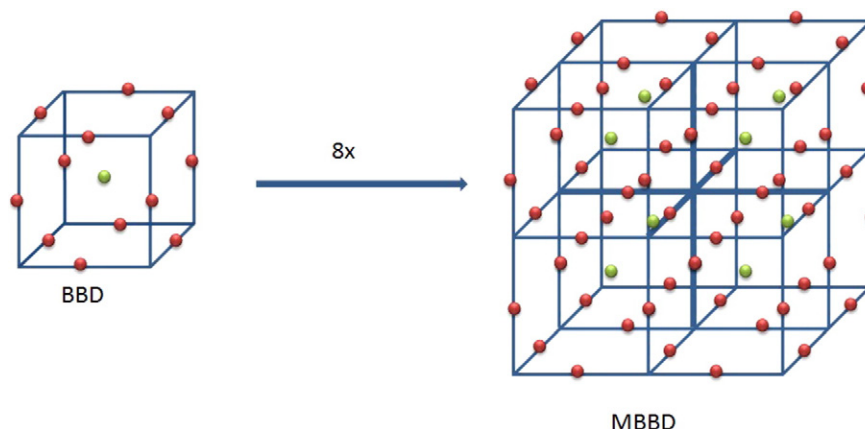


Fig. 1. Multiple Box–Behnken experimental design (MBBD).

**Table 1**

Mean square error (MSE) calculated for each ANN at different number of neurons on the hidden layer.

Number of neurons	Methanol (MSE)	Ethanol (MSE)	i-Propanol (MSE)
2	7.03E-02	2.69E-02	7.80E-02
5	3.60E-02	9.41E-03	4.54E-03
10	3.85E-03	3.68E-03	1.27E-03
20	2.79E-03	1.17E-03	3.72E-04
30	3.06E-04	2.71E-04	9.18E-04
40	1.47E-03	3.09E-03	7.22E-04
50	<b>1.94E-04</b>	8.76E-04	1.39E-04
60	2.63E-04	<b>9.49E-05</b>	<b>4.60E-05</b>
70	1.42E-03	7.93E-04	8.88E-04
80	1.05E-03	1.26E-03	2.70E-03
90	1.26E-03	4.14E-04	1.11E-04
100	1.76E-03	6.00E-04	3.19E-03

Note: The numbers in bold are the minimum MSE obtained.

proportion, the carrier flow rate, and the acetylene/air ratio that controls flame stoichiometry. The experimental setup was the same employed in a previous work [6].

### 3.1. Multiple Box–Behnken experimental design (MBBD)

According to the multivariate approach for optimization, all variables should be changed at the same time. In this work, BBD was applied

to three parameters that represent an experimental run. With a simple BBD experiment, the whole experimental domain is sampled with thirteen experimental runs which seem not enough for a correct model building. Then, to effectively improve the number of sampling points, the experimental domain was divided into eight equal quadrants, and a BBD was performed in each one of them as shown in Fig. 1, being the volumes of both cubes (BBD and MBBD) the same as stated before. Then a total of 62 experimental runs for each alcohol mixture was performed for modeling with neural networks. This is a much more economic approach compared to the 125 runs required for a five-level full factorial design which is a must choice for solving complex problems involving high-order polynomials.

### 3.2. Analysis by least squares

The ANOVA tests applied to the factors and responses data demonstrated that cubic models could fit the three responses (EtOH, MeOH, and i-PrOH). The associated probability values ( $p$ ) obtained for the models were less than 0.001 for the three cases, while the corresponding  $p$  values for the lack of fit test for the three models were larger than 0.500, thus indicating the significance of the models. Notice that the probability value is computed assuming that the null hypothesis is true and so, the lower the probability value, the stronger the evidence that the null hypothesis is false. Traditionally, the null hypothesis is rejected if the probability value is below 0.05. Nevertheless, some

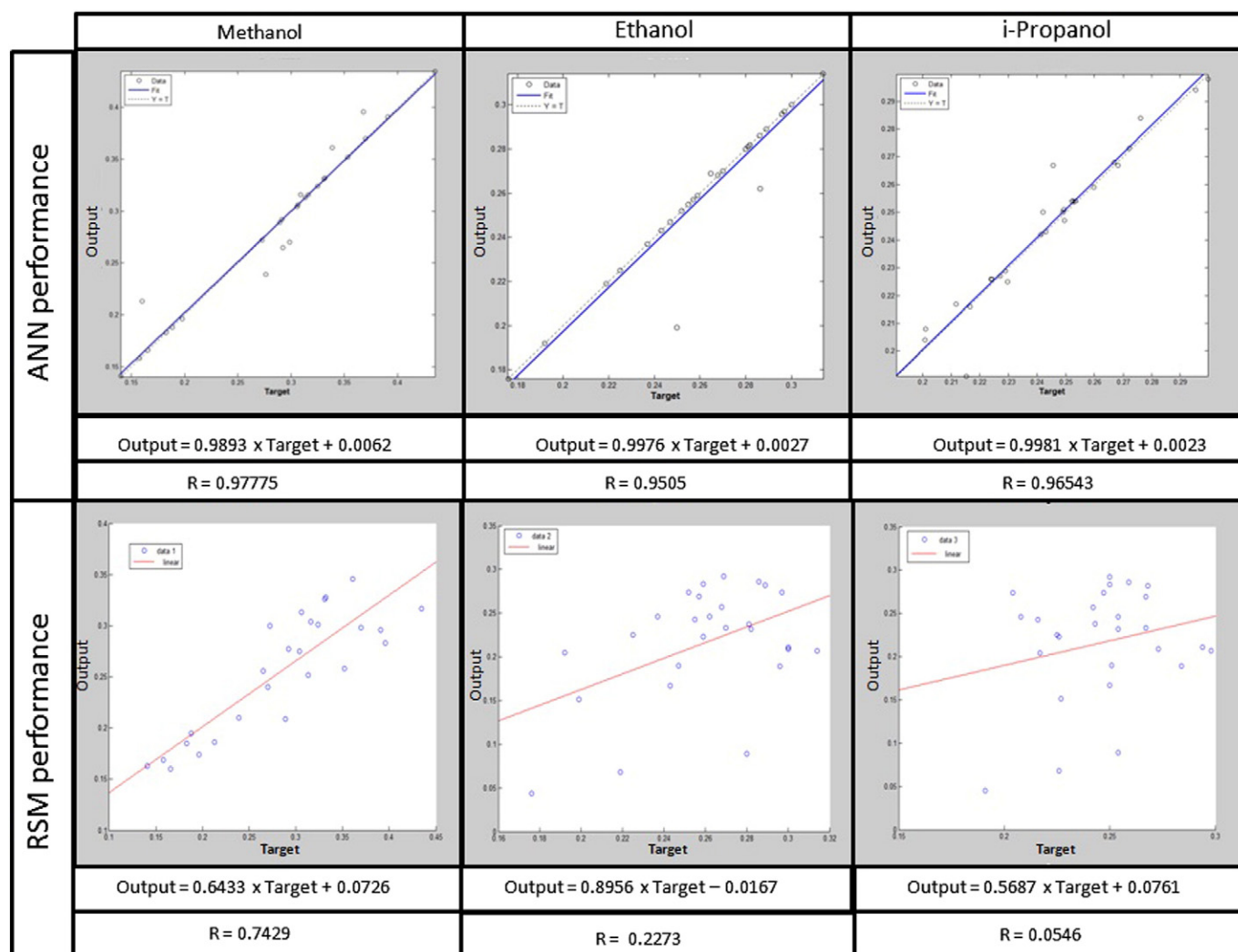


Fig. 2. ANN and RSM performances: output predicted by ANN against the target values obtained from experimental data and output predicted by RSM against target values obtained from experimental data.



statistical results were not satisfactory: the adjusted  $R^2$  obtained were 0.824, 0.852, and 0.837 for EtOH, MeOH, and i-PrOH, respectively, implying that these models could explain only ca. 85% of the variability in the responses, with the remaining 15% explained by the residue. This fact could be indicative that the models are not suitable for prediction purposes.

### 3.3. Artificial neural network training and prediction

Back-propagation neural network was applied for modeling the systems response and all the neurons had sigmoidal transfer functions.

The architecture of the net was designed using three factors (solvent flow rate, solvent concentration, and acetylene flow rate) as each unit of input layer. The output layer was composed of the peak height observed as a response variable.

Typically one hidden layer is used in a network. In the present work, just one hidden layer was used because no significant improvement in performance was observed by increasing the number of hidden layers.

Several iterations were conducted with different numbers of neurons of hidden layer to determine the optimal ANN structure. The optimum number of neurons in the hidden layer was iteratively determined by changing the number of neurons from 2 to 100. We use the mean square error (MSE) to decide which number of neurons in the hidden layer is the best. The results for the three neural networks are shown in Table 1.

Afterwards, in order to assure the prediction capability of ANN, the results were compared to 28 experimental runs specially measured around the maxima found for the different carrier flow rates. In doing

that, output values were plotted against the corresponding observed values. The results are shown in Fig. 2.

The results show that predicted data obtained by LS have a low concordance with the experimental measurements (see Fig. 2). However, despite a few outliers, there is a very good agreement between the ANN predictions and the experimental data (Fig. 2) as revealed by the low MSE values, slopes and correlation coefficients close to 1 and intercepts near zero. Therefore, in contrast with LS-RSM model, ANN could be accepted as a precise prediction for modeling the analytical sensitivity of magnesium by TS.

Fig. 3 shows some of the results predicted by ANN. The response surfaces obtained at different sample flow rates (ranging from 0.4 to 1.4 mL·min<sup>-1</sup>) for each one of the three alcohols are displayed as 3D surfaces and contour plots. The X, Y, and Z axis represent the %v/v of alcohol, the acetylene flow rate (L min<sup>-1</sup>), and the peak height, respectively.

### 3.4. Analysis of the optimal conditions

Figs. 3 and 4a show that as long as the carrier flow is increased, maximum sensitivity is reached at lower percentages of organic solvent. It can be noticed that an increment in the carrier flow increases the absolute amount of alcohol that reaches the furnace. In this way, the percentage alcohol/water can be reduced keeping constant the total amount of organic solvent with no harm for sensitivity. Fig. 4 (down) shows the influence of carrier flow rate on the moles of oxygen consumed in a combustion by the solvent per minute. With the same argument as before, as long as the flow rate increases, alcohols with more carbon atoms in

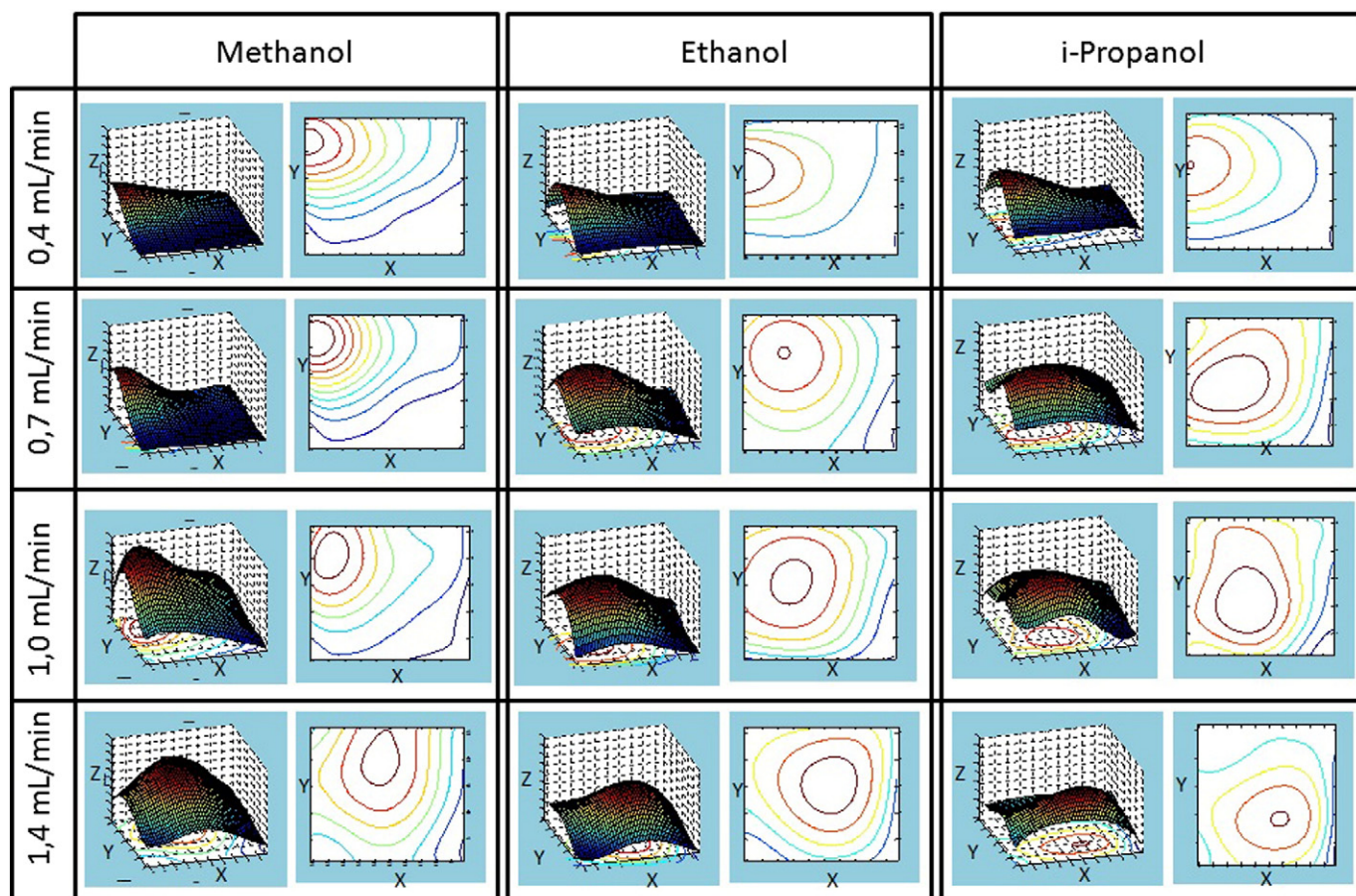
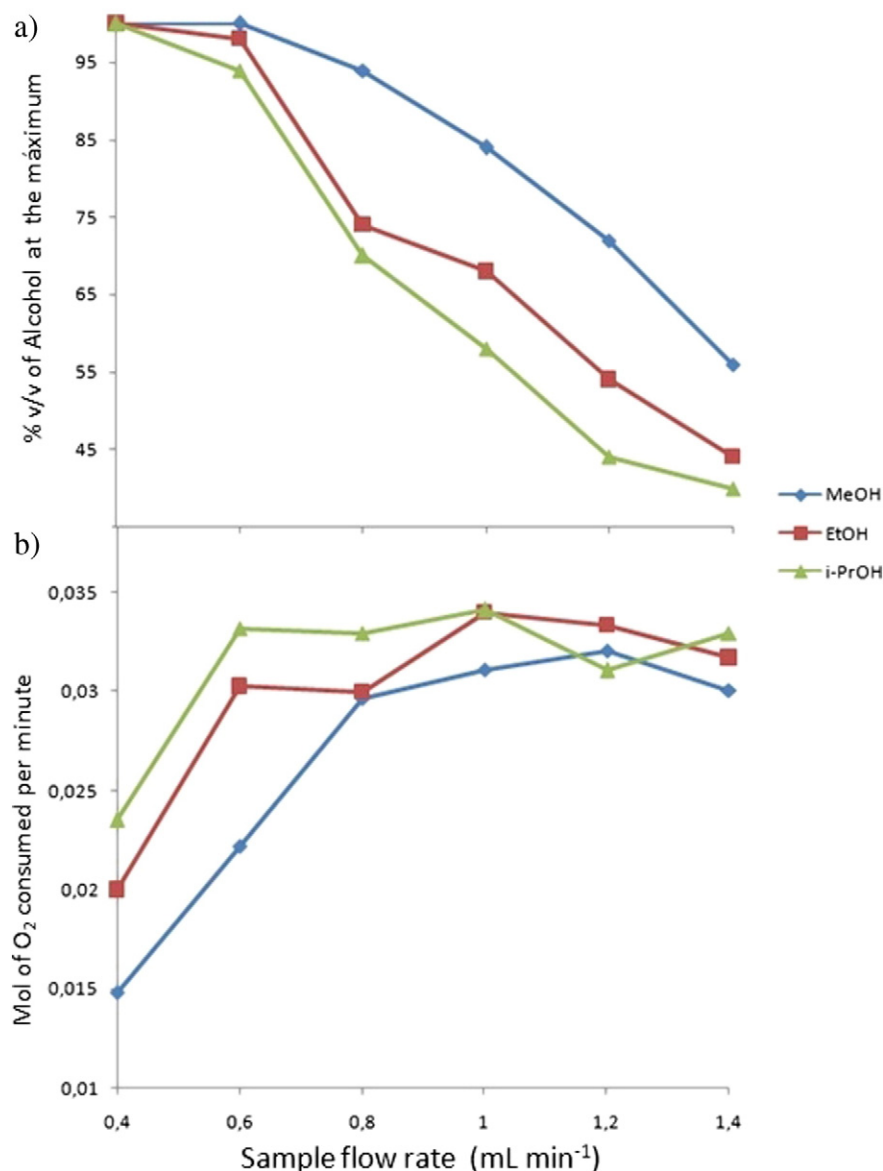


Fig. 3. 3D surfaces and contour plots predicted by ANN. X is %v/v of alcohol, Y is acetylene flow rate (L min<sup>-1</sup>) rate, and Z is peak height (arbitrary units).



**Fig. 4.** a) Solvent percentage in the mixture vs. sample flow rate: influence on optimal sensitivity; b) moles of oxygen per minute consumed in a combustion by each alcohol mixture vs. sample flow rate.

its molecule reach their maximum at lower organic fractions of the solvent (Fig. 4b).

Fig. 5 took into account the organic proportion of the solvent in the mixture and the acetylene flow rate under the optimal conditions established for each one of the response surfaces. Each point corresponds to the maximum at a certain sample flow rate. Even there is not a fixed value for all the maxima, the tendency shows that a full richer flame produces a more suitable environment for Mg atomization when using a solvent with methanol (one carbon) and that a fuel leaner flame is advisable when the number of carbon atoms is increased (ethanol and i-propanol).

Fig. 6 shows the analytical sensitivity for Mg (expressed as peak height) under optimal solvent proportion and flame stoichiometry at different sample flow rates. The inset figure shows the influence of the solvent proportion of the carrier on the droplet size measured as Sauter Mean Diameter (SMD).

The maxima in Fig. 6 can be attributed to a compromise situation: on one hand, the signal increases as long as the flow rate increases, and in the other hand, the amount of sprayed solvent grows, promoting a decrease in temperature of the furnace and, thus, a lower generation of atomic

vapor. Regarding the droplet diameter (inset Fig. 6), the higher the organic proportion of the mixture, the smaller the droplet size and the better the desolvation/atomization dynamics and therefore the sensitivity.

#### 4. Conclusions

The studies show that the combination between experimental design and ANN has been successful for predicting the behavior of magnesium when determined by TS-FFAAS under different operational variables.

ANN-RSM has revealed itself as a much better alternative for prediction when compared to LS-RSM in this particular system. Moreover, the economy in experimental runs allows saving time, reagents, and thus, costs.

Regarding the influence on the analytical sensitivity in TS-FFAAS with magnesium as leading case, it has been shown that the optimal conditions arise from a proper combination of the main operational variables which is better attained through the multivariate approach rather than the one variable at a time.

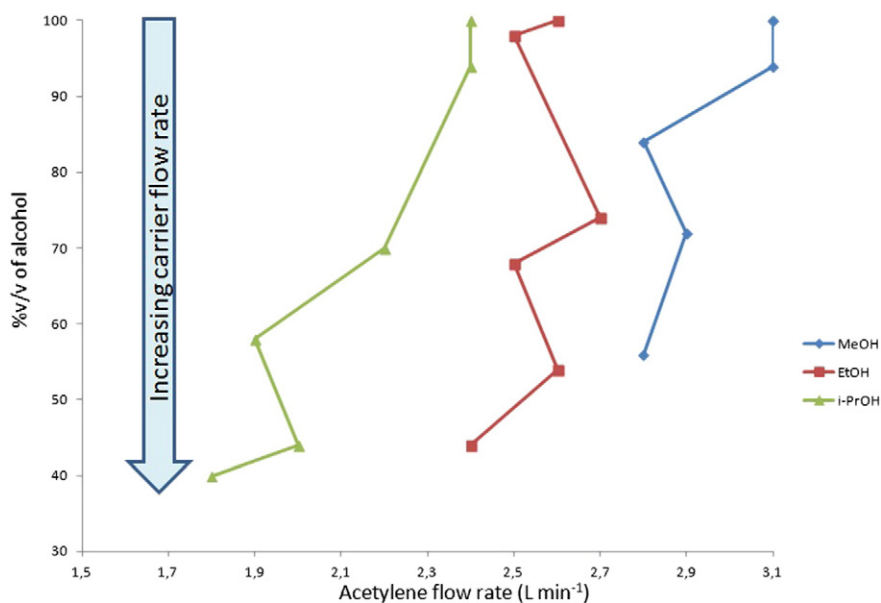


**Fig. 5.** Optimal conditions at different sample flow rates. Each point shows the maximum sensitivity at a given sample flow rate. Flow rates increase downwards (see arrow).

We consider that these results could be a useful instrument and a route to follow for attaining the determination via TS of other elements not tested up to date, broaden in this way the analytical capabilities of this technique.

#### Conflict of interest

The authors declare that they have no conflict of interest.

#### Acknowledgments

The authors gratefully acknowledge financial support from the following agencies and organizations: Ministerio de Ciencia, Tecnología e Innovación Productiva (MinCyT) Argentina, Consejo Nacional

de Investigaciones Científicas y Técnicas (CONICET) Argentina; Universidad de Buenos Aires and Universidad Nacional del Litoral.

#### References

- [1] A. Gáspár, H. Berndt, Thermospray flame furnace atomic absorption spectrometry (TS-FF-AAS)—a simple method for trace element determination with microsamples in the  $\mu\text{g/l}$  concentration range, *Spectrochim. Acta B* 55 (2000) 587–597.
- [2] M.L. Brancalion, E. Sabadini, M.A.Z. Arruda, Description of the thermospray formed at low flow rate in thermospray flame furnace atomic absorption spectrometry based on high-speed images, *Anal. Chem.* 79 (2007) 6527–6533.
- [3] M.A.Z. Arruda, E.C. Figueredo, Atomic spectrometry based on metallic tube atomizers heated by flame: innovative strategies from fundamentals to analysis, *Spectrochim. Acta B* 64 (2009) 477–481.
- [4] K. Miranda, E.R. Pereira-Filho, Potentialities of thermospray flame furnace atomic absorption spectrometry (TS-FF-AAS) in the fast sequential determination of Cd, Cu, Pb and Zn, *Anal. Methods* 1 (2009) 215–219.

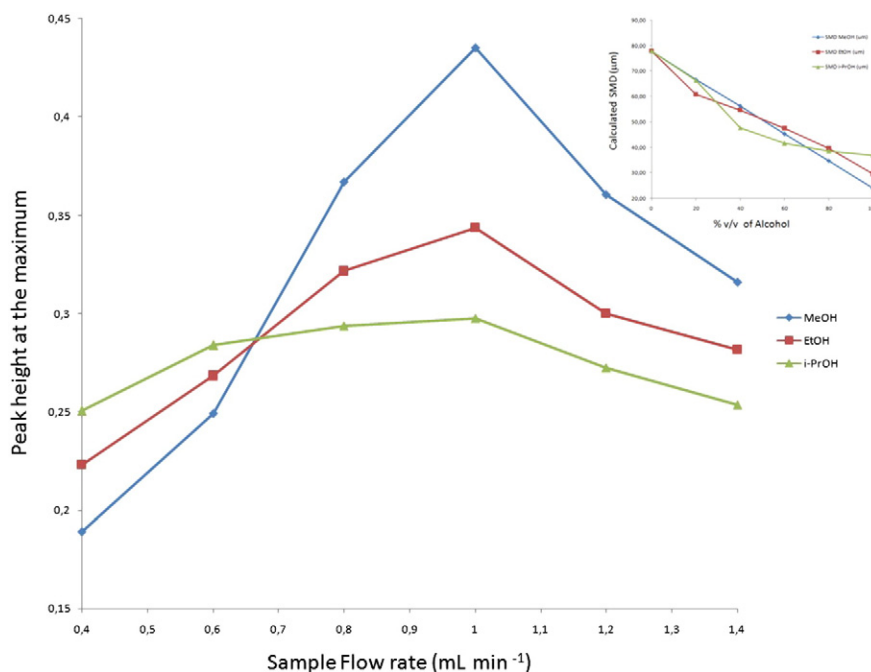


**Fig. 6.** Peak height at optimal conditions for the different sample flow rates. The inset figure shows the calculated Sauter Mean Diameter (SMD) (Ref. [6]) vs. the % of solvent for each one of the three alcohols.

- [5] E. Morzan, O. Piano, J. Stripeikis, M. Tudino, Evaluation of quartz tubes as atomization cells for gold determination by thermospray flame furnace atomic absorption spectrometry, *Spectrochim. Acta B* 77 (2012) 58–62.
- [6] E. Morzan, J. Stripeikis, M. Tudino, Towards broadening thermospray flame furnace atomic absorption spectrometry: influence of organic solvents on the analytical signal of magnesium, *Anal. Chem. Res.* 4 (2015) 1–7.
- [7] L. Vera-Candioti, M. Cámara, M. Dezan, H. Goicoechea, Experimental design and multiple response optimization. Using the desirability function in analytical methods development, *Talanta* 124 (2014) 123–138.
- [8] R. H. Myers, D. C. Montgomery in *Response Surface Methodology, Process and Product Optimization using Designed Experiments*, Ed. Wiley & Sons, New York, 3rd ed. 2009.
- [9] G. Dingstad, B. Egelanddal, T. Naes, Modeling methods for crossed mixture experiments—a case study from sausage production, *Chemom. Intell. Lab. 66* (2003) 175–190.
- [10] K.M. Lee, D.F. Gilmore, Formulation and process modeling of biopolymer (polyhydroxyalkanoates: PHAs) production from industrial wastes by novel crossed experimental design, *Process Biochem.* 40 (2005) 229–246.
- [11] K. Adinarayana, P. Ellaiah, B. Srinivasulu, R. Bhavani Devi, G. Adinarayana, Response surface methodological approach to optimize the nutritional parameters for neomycin production by *Streptomyces marinensis* under solid-state fermentation, *Process Biochem.* 38 (2003) 1565–1572.
- [12] S.G. Prapulla, Z. Jacob, N. Chand, D. Rajalakshmi, N.G. Karanth, Maximization of lipid production by *rhodotorula gracilis* CFR-1 using response surface methodology, *Biotechnol. Bioeng.* 40 (1992) 965–970.
- [13] I.C. Roberto, S. Sato, I.M. de Mancilha, M.E.S. Taqueda, Influence of media composition on xylitol fermentation by *Candida guilliermondii* using response surface methodology, *Biotechnol. Lett.* 17 (1995) 1223–1228.
- [14] Y.T. Liu, C.N. Long, S.X. Xuan, B.K. Lin, M.N. Long, Z. Hu, Evaluation of culture conditions for cellulase production by two *Penicillium decumbens* under liquid fermentation conditions, *J. Biotechnol.* 1365 (2008) S328.
- [15] G. Dingstad, F. Westad, T. Naes, Three case studies illustrating the properties of ordinary and partial least squares regression in different mixture models, *Chemom. Intell. Lab.* 71 (2004) 33–45.
- [16] G.F. Piepel, Modeling methods for mixture-of-mixtures experiments applied to a tablet formulation problem, *Pharm. Dev. Technol.* 4 (1999) 593–606.
- [17] P.J. Brandvik, Statistical simulation as an effective tool to evaluate and illustrate the advantage of experimental designs and response surface methods, *Chemom. Intell. Lab.* 42 (1998) 51–61.
- [18] N. Ortega, S.M. Albillos, M.D. Busto, Application of factorial design and response surface methodology to the analysis of bovine caseins by capillary zone electrophoresis, *Food Control* 14 (2003) 307–315.
- [19] C. Severini, A. Baiano, T. De Pilli, R. Romaniello, A. Derossi, A. Lebensm, Prevention of enzymatic browning in sliced potatoes by blanching in boiling saline solutions, *Wiss. Technol.* 36 (2003) 657–665.
- [20] J.V. Nardi, W. Acchar, D. Hotza, Enhancing the properties of ceramic products through mixture design and response surface analysis, *J. Eur. Ceram. Soc.* 2004 (24) 375–379.
- [21] F. Abnisa, W.M.A. Wan Daud, J.N. Sahu, Optimization and characterization studies on bio-oil production from palm shell by pyrolysis using response surface methodology, *Biomass Bioenergy* 35 (2011) 3604–3616.
- [22] P.C. Giordano, H.D. Martínez, A.A. Iglesias, A.J. Beccaria, H.C. Goicoechea, Application of response surface methodology and artificial neural networks for optimization of recombinant *Oriza sativa* non-symbiotic hemoglobin 1 production by *Escherichia coli* in medium containing byproduct glycerol, *Bioresour. Technol.* 101 (2010) 7537–7544.
- [23] E. Betiku, S.S. Okubikawi, S.O. Ajala, O.S. Odelele, Performance evaluation of artificial neural network coupled with generic algorithm and response surface methodology in modeling and optimization of biodiesel production process parameters from shea tree (*Vitellaria paradoxa*) nut butter, *Renew. Energy* 78 (2015) 408–417.
- [24] J. Prakash Maran, B. Priya, Comparison of response surface methodology and artificial neural network approach towards efficient ultrasound-assisted biodiesel production from muskmelon oil, *Ultrason. Sonochem.* 23 (2015) 192–200.
- [25] M. Sabonian, M.A. Behnajady, Artificial neural network modeling of Cr(VI) photocatalytic reduction with TiO<sub>2</sub>-P25 nanoparticles using the results obtained from response surface methodology optimization, *Desalin. Water Treat.* (2015), <http://dx.doi.org/10.1080/19443994.2014.963161> (article in press).
- [26] S.F. Silva, C.A.R. Anjos, R.N. Cavalcanti, R.M.D.S. Celeghini, Evaluation of extra virgin olive oil stability by artificial neural network, *Food Chem.* 179 (2015) 35–44.
- [27] K.M. Desai, S.A. Survase, P.S. Saudagar, S.S. Lele, R.S. Singhal, Comparison of artificial neural network (ANN) and response surface methodology (RSM) in fermentation media optimization: case study of fermentative production of scleroglucan, *Biochem. Eng. J.* 41 (2008) 266–273.